Electronic Supplementary Material (ESI) for Sustainable Energy & Fuels.

Supplementary information

One-pot reductive liquefaction of sawdust to renewables over $MoOx\text{-}Al_2O_3$ variations: an insight into structure-activity relationships.

Muhammad Abdus Salam[a], Quoc Khanh Tran[a], Phuoc Hoang Ho[a], You Wayne Cheah[a], Joanna Wojtasz-Mucha[a], Christian Kugge[b] Elham Nejadmoghaddam[a], Louise Olsson [a], and Derek Creaser [a]

[a] *Chemical Engineering, Competence Centre for catalysis, Chalmers University of Technology, SE-412 96 Gothenburg, Sweden*

[b] *SCA R&D Centre, Sundsvall, Sweden*

Table S1. Overview of a literature survey corresponding to biomass conversion over MoOx containing catalysts

Catalyst	Mult-stage or Direct conversion*	Application	Highlights	Ref.
Fe-Mo/HZSM-5(38)	Multi-Stage	Pyrolysis and catalytic upgrading of sawdust using pyrolytic (550°C)/catalytic reactor (500°C)in two stages. Sawdust to catalyst ratio=3:1	Highest organic phase bio-oil yield (20.74 wt.%) for 1wt.%Mo-1wt.%Fe /HZSM-5(38) combination due to well balanced acidity.	[1]
NiMo-HZSM-5(Si/Al=25)	Multi-Stage	Hydropyrolysis (700°C) and catalytic vapor hydrotreatment of sawdust using two-stage fixed bed reactor (5 MPa H_2, 350°C)	1% Ni 3% Mo-HZSM-5 shows best catalytic activity. 23.9 wt.% of bio-oil with a high (~72%) aliphatic hydrocarbon selectivity. Mo-drives the formation of aromatic intermediates pool while Ni facilitates hydrogenation and HDO.	[2]
Mo-Cu/HZSM (Si/Al=30)	Multi-Stage	Catalytic pyrolysis of pine sawdust	3% Mo 3%Cu /HZSM-5 enables higher C_6-C_{12} fraction formation owing to optimum Brønsted acidic sites. Also, the presence of CuO helps disperse MoO_x over HZSM-5. However, reported -25% solid bio-char.	[3]
Mo, V. Ag, Pd over SBA-15/HZSM-5	Multi-Stage	Sawdust and waste tyre coprocessing in a stainless steel tube setup (pyrolysis followed by catalytic upgrading)	Bio-oil produced having 40 wt.% sawdust and 60 wt.% tyre over Ag/SBA-15 shows properties similar to diesel fuel.	[4]
Ni-Mo/γ-Al_2O_3	Multi-Stage	Hydropyrolysis (500℃) and vapor upgrading (300-400℃) of poplar wood using microreactor/fluidized bed system	Oil phase yield of 6-8% having high selectivity for C_{8+} aliphatics (solid char~32%). Experimental and theoretical insights for the carbon-carbon couping reaction occruing during biomass hydropyrolysis.	[5]

MoO_3/TiO_2 and MoO_3/ZrO_2	Multi-Stage	Catalytic fast pyrolysis of Pine at 500 °C and ≤0.75 bar H_2 pressure	~27% overall C-yield composed of olefins and aromatic hydrocarbons (char~39%). Biomass to catalyst ratio greatly affects the product selectivites. Surface Mo-species (Mo^{+3} and Mo^{+5}) facilitates the observed reactivity.	[6]
MoOx/KIT-5	Multi-Stage	Catalytic fast pyrolysis of yellow pine (500°C)	High selectivity of furans and phenols for Mo-loading of 2.5 and 3.7 wt.% over KIT-5 due to better dispersion of Mo-sites which prevents sintering	[7]
Pt/TiO_2 , MoO_3/TiO_2 Industrial MoO_3/Al_2O_3 (industrial)	Multi-Stage	Fast pyrolysis (530°C) of Wheat straw and catalytic upgrading (400-450°C, 50 or 90 vol.% H_2, ~atmospheric HDO) of pyrolysis vapor.	10 wt.% MoO_3/TiO_2 shows similar deoxygenation activity, carbon yield and energy recovery to that of 0.5wt%Pt/TiO_2 at 50 vol% H_2. Industrial Mo/Al_2O_3 on the other hand shows high gas and coke yields (due to high acidity and catalytic cracking) and lower oil yield (less hydrogenation activity).	[8]
Al_2O_3-based. solid acid catalyst (SA1), W and M-based reducible metal oxide (RMO1, RMO2), Fe-based mixed metal oxide (MMO1)	Direct	Reactive catalytic fast pyrolysis (RCFP) of loblolly pine sawdust using fluidized bed reactor under H_2 at atmospheric pressure	High deoxygenation activity over Mo-based catalyst yields bio-crude rich in hydrocarbon (c4+ organics~43% at 80 vol% H_2, and 450°C) and low oxygen content (~6.2 wt.%). Char amount of ~30 wt.%	[9]
MoZn/HZSM-5(Si/Al = 30) MoO_3/HZSM-5 Mo_2C/HZSM-5 MoAg/HZSM-5	Multi-Stage	Co-pyrolysis of torrefied switchgrass (230 or 270°C, 30 min) under methane/He atmosphere.	Aromatic hydrocarbon yield of (39%) over MoZn/HZSM-5 under CH_4 atmosphere, at 700°C. Bimetallic catalysts effective in activating both methane and pyrolyzed bio-oil than monometallic Mo-catalysts.	[10]
Bulk MoO_3 (Sigma Aldrich)	Multi-Stage	Pyrolysis (500°C) and ex-situ catalytic	High yield of linear alkanes (C_1-C_6) and	[11]

		upgrading using cellulose, lignin and corn stover (300-400°C, near atmospheric H_2 pressure, P_{total} =1.8 bar)	aromatics (up to ~70-90% C of pyrolysis vapor. The yield of char from cellulose, lignin, and corn stover were 10.1 C%, 55.5 C%, and 43.0 C% respectively.	
5 wt% Pt–2.5 wt% Mo/MWCNT	Multi-Stage	Fast-hydropyrolysis (~500°C) coupled with catalytic HDO (~300-350°C)	~73% C as C_1–C_{8+} hydrocarbon yield using cellulose feedstock (char ~2 wt% of feed). ~54% C as C_1–C_{8+} hydrocarbon yield from poplar (char ~29% C, ~18.4 wt% of feed) Pt-acts as hydrogenation function and Mo as oxophillic promoter.	[12]
MoO_2/C (10 wt.%), MoO_3/C	Direct	Reductive catalytic fractionation (RCF) of Miscanthus (and additionally Triarrhena, Floridulus, Sorghum stem and Corncob) sawdust using methanol and H_2 (10-40 atm), 220-280 °C, 4 h.	26.4 wt.% of phenolic monomers via selective hydrogenolysis of miscanthus sawdust lignin interestingly with high sugar retention as solid/carbohydrate pulp (~87%). MoO_3/C is less reactive than MoO_2/C	[13]
NiMo-Oxide, Reduced, sulfide and Pd/C, Pd/Al2O3, Bulk MoS_2	Multi-Stage	Hydrotreatment of liquefied wood samples (debarked sawdust of European spruce and European silver fir) using glycerol and diethylene glycol (1:1 by mass) as solvent in autoclave using continuous H_2 feed at 300 °C and 8 MPa	Sulfided NiMo/Al_2O_3 shows high HDO activity, better liquid yield, low viscosity and high GCV of the upgraded product.	[14]
NiMo/Al_2O_3, Pd/Al_2O_3, and Zeolite Y	Direct	Direct solvolysis and hydro-treatment of oak, fir and beech sawdust employing H-donor solvents (tetralin, phenol and	Highest yield of liquefied-oil, HDO products, and lowest tar (<10%) using sulfided NiMo-Al_2O_3	[15]

		glycerol). Sawdust to solvent mass ratio of 1:4, 10 wt.% catalyst (based on dry sawdust), 2-8 MPa H_2, 300-350 °C		

**Direct conversion: catalyst and biomass comes in direct contact, Multi-stage: Pyrolysis vapor formation and subsequent catalytic upgradation in steps.*

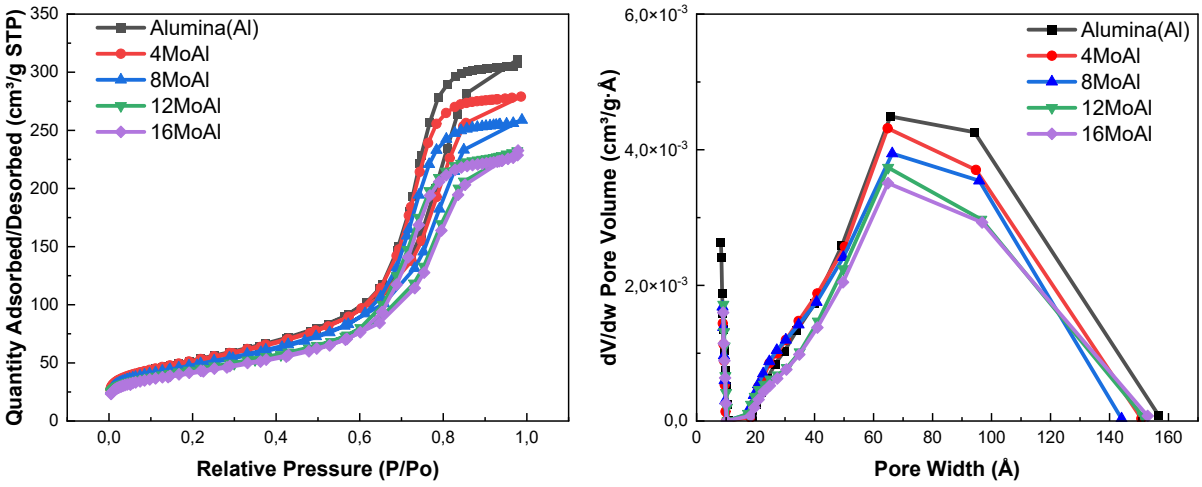

Fig.S1. Nitrogen physisorption isotherms and pore size distribution for the synthesized catalysts (varying Mo-loading over γ-Al_2O_3).

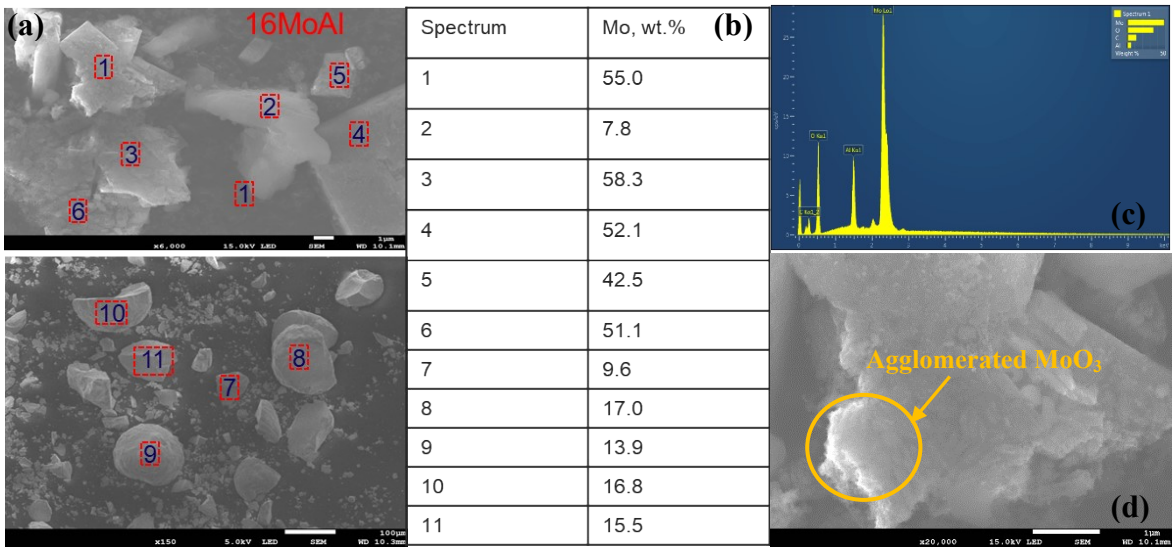

Spectrum	Mo, wt.%
1	55.0
2	7.8
3	58.3
4	52.1
5	42.5
6	51.1
7	9.6
8	17.0
9	13.9
10	16.8
11	15.5

Fig.S2. SEM-EDX data showing the (a) analyzed area, (b) variation of Mo-contents (spectrum 1-11) (c) EDX of spectrum 1 and (d) presence of agglomerated MoO_3 over 16MoAl.

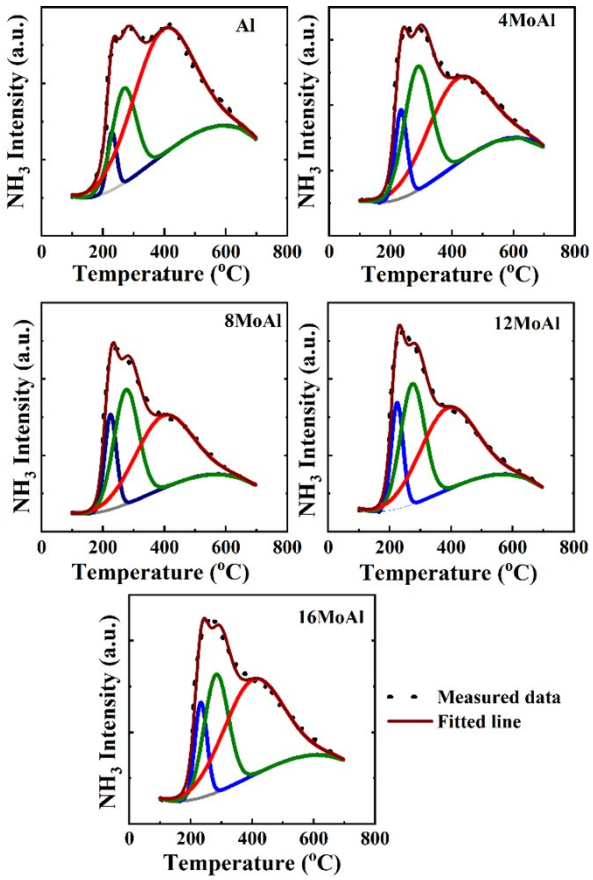

Fig.S3. Deconvolution of NH3-desorption profile obtained for Alumina (Al), 4MoAl, 8MoAl, 12MoAl, and 16MoAl.

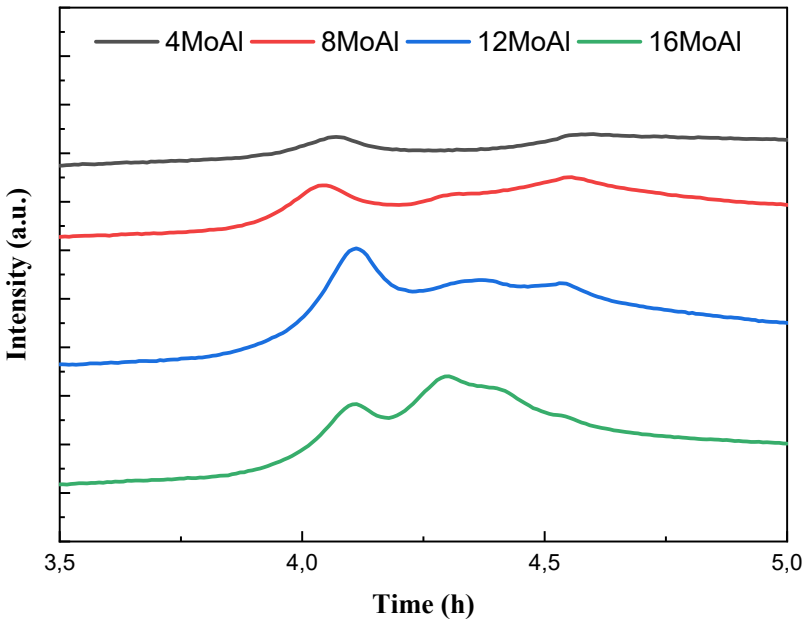

Fig.S4. H_2 TPR profile for the synthesized catalysts with varying Mo-loading on γ-Al_2O_3 showing the consumption of H_2 vs time data.

Table S2. H_2 consumption during H_2-TPR

Catalyst	H_2 consumption during TPR, µmolg^{-1}
4MoAl	92
8MoAl	215
12MoAl	405
16MoAl	492

The overall mass balance for each experiment was found to be in the range of 40-83 wt.% based on the dry sawdust charged into the reactor and the GC-detectable products. A low value of mass balance is due to oligomerization products (GC undetectable), and some loss of material in the reactor system (e.g. headspace).

Table S3. Overall mass balance for the reductive liquefaction of sawdust over reduced xMoAl catalysts at 340-400 °C, 35 bar H_2 (@25°C, and 4 h in a batch reactor.

Entry	Catalyst	Temperature (°C)	H_2 conversion (%)	GC detectable bio-oil Products, wt.%	Oxygen as H_2O, wt. %	Yield of Gas-phase products, wt.%	Solid residue, wt.%	Mass balance, wt.%
1	Blank	340	-	8.9	6.7	1.2	23.4	40.3
2	Al			-	-	-	22.7	-
3	4MoAl		-	16.2	21.7	8.6	16.2	62.7
4	8MoAl		12.2	24.8	19.4	8,3	13.6	66.1
5	12MoAl		-	24.1	22.1	-	14.1	-
6	16MoAl		-	26.5	19.7	13.5	16.5	74.7
7	8MoAl	370	-	-	-	-	10.3	-
8	8MoAl	400	25.8	29.2	19.7	14.6	6.5	70.1
9	8MoAl[b]			-	-	-	4.9	-
10	8MoAl[c]		31.2	39.4	16.3	17.4	9.7	82.8

[b]Experiment with sawdust particle size <100µm, [c]Experiment with sawdust:catalyst mass ratio of 10:1. All other experiments were run with the sawdust particle size of <500 µm and sawdust:catalyst mass ratio of 3:1.

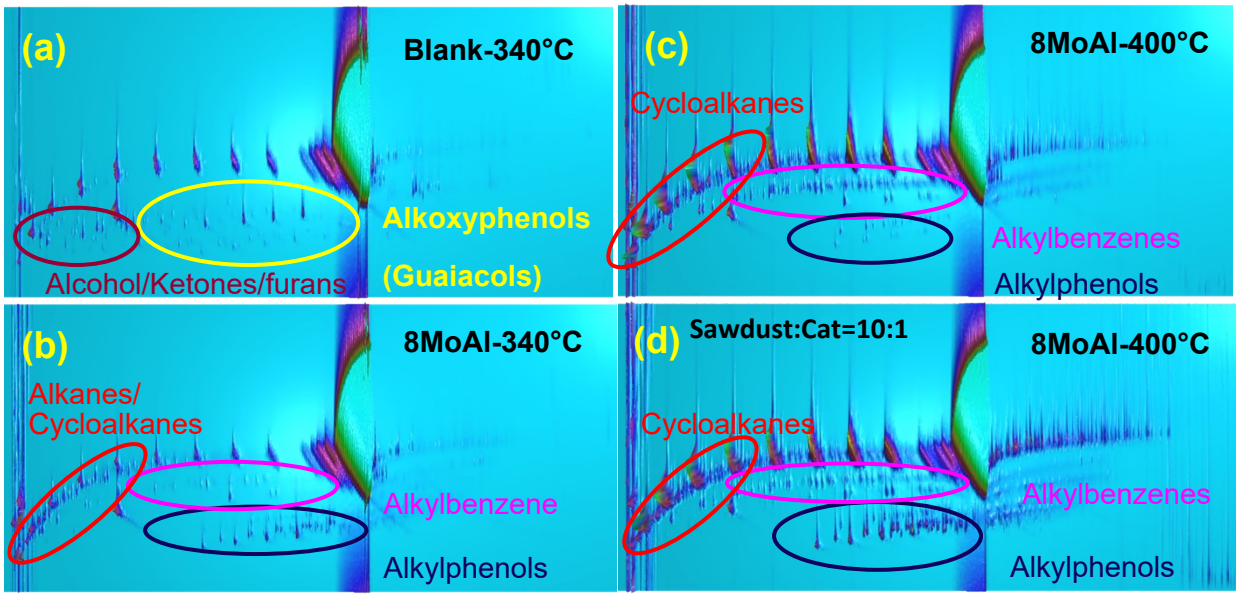

Fig.S5. 2D GCxGC chromatogram of the liquid phase products evolved from the reductive liquefaction of sawdust over 8MoAl for sawdust to catalyst ratio of 3:1 (a-c) and for 10:1 ratio (d)

Table S4a. The list of compounds in liquefied phase from reductive liquefaction of sawdust over 8MoAl identified via 2D GCxGC analysis

Retention I (min)	Retention II (sec)	Compound Name
4.34	0.56	1-Butanol, 3-methyl-
4.34	1.20	1-Butanol, 3-methyl-
4.92	0.68	2(3H)-Furanone, dihydro-3,5-dimethyl-
5.00	1.16	2-Propanone, 1-methoxy-
5.17	1.60	n-Hexane
5.67	1.20	Cis-bicyclo[4.2.0]octane
6.25	0.88	Cyclobutene, 3,3-dimethyl-
6.67	0.92	2-Butanone, 3-methoxy-3-methyl-
7.00	1.08	2-Penten-1-ol, 2-methyl-, (Z)-
7.34	1.08	Cyclopentane 4,4 dimethyl
7.59	1.12	1,4-Hexadiene, 4-methyl-
7.84	1.24	Methyl cyclohexane
8.09	1.04	Furan, 2-ethyl-
8.09	1.28	Cyclopentane, ethyl-
8.42	1.08	Tetrahydropyran
8.59	1.24	Cyclopropane, trimethylmethylene-
8.84	1.28	2,3-Hexadiene, 2-methyl-
9.00	0.88	1-Butanol
9.50	1.36	(E)-2-Butenylcyclopropane
10.09	1.52	2-Hexene, 3,5-dimethyl-
10.25	1.48	3-Hexene, 2,3-dimethyl-
10.42	1.52	2-Methyl-1,5-heptadiene (c,t)
10.67	1.24	Toluene
10.75	1.56	Cyclohexene, 1 ethyl
11.09	1.36	trans-(2-Ethylcyclopentyl)methanol
11.09	1.60	1-Ethyl-5-methylcyclopentene

11.50	1.64	Hepten-2-yl tiglate, 6-methyl-5-
12.34	1.64	1-Propylcyclopentene
14.92	1.52	Benzene, 1,3-dimethyl-
14.92	1.88	3-Heptene, 2,6-dimethyl-
15.17	1.88	1,3-Hexadiene, 3-ethyl-2-methyl-
15.42	1.52	Ethylbenzene
15.42	1.88	Cyclohexane,1 methyl 4 (2 hydroxyethyl)
15.92	1.92	1,3-Hexadiene, 3-ethyl-2-methyl-
16.34	2.00	Cyclohexane, propyl-
16.67	1.96	1,3-Hexadiene, 3-ethyl-2-methyl-
17.17	1.92	Cyclopentnecarboxaldehyde, 2-methyl-3 methylene
17.75	1.96	Cyclohexene,3-propyl-
18.09	1.68	Benzene, (1-methylethyl)-
18.17	2.04	Cyclohexene,1-propyl-
18.59	2.08	Bicyclo[4.1.0]heptane, 3,7,7-trimethyl-
18.92	2.08	1,4-Hexadiene, 3-ethyl-4,5-dimethyl-
19.67	1.48	Anisole (Internal Standard)
19.84	1.72	Benzene, propyl-
20.25	2.12	cis-1,2-Cyclohexanedimethanol
20.34	1.68	Benzene, (1-methylethyl)-
20.42	2.12	Cyclooctene, 1,2-dimethyl-
20.59	2.12	di-t-Butylacetylene
21.00	2.12	7-Oxabicyclo[4.1.0]heptane, 3-oxiranyl-
21.59	1.72	Benzene, 1-ethyl-2-methyl-
22.50	1.76	Benzene, (1-methylethyl)-
23.34	2.20	7-Propylidene-bicyclo[4.1.0]heptane
23.59	2.16	Cyclohexane, 1-butenylidene-
23.75	2.20	Neodihydrocarveol
24.00	2.20	Cyclohexene, 4-methyl-1-(1-methylethyl)-
24.42	2.20	3-Methyl-trans-3a,4,7,7a-tetrahydroindane
24.42	1.76	Benzene, 1-ethyl-3-methyl-
24.75	2.23	Bicyclo[3.1.1]heptane, 6,6-dimethyl-3-methylene-
25.25	1.80	Benzaldehyde, 4-(1-phenyl-2-propenyloxy)-
25.50	1.84	Benzene, 1-methyl-3-propyl-
25.92	1.88	Benzene, 1,2-diethyl-
26.67	1.84	Benzene, 1-methyl-4-propyl-
26.92	2.23	3,6-Octadien-1-ol, 3,7-dimethyl-, (Z)-
27.42	1.88	Benzene, 2-ethyl-1,4-dimethyl-
27.84	1.84	1-Phenyl-1-butene
28.09	1.84	Benzene, 1-ethenyl-4-ethyl-
28.34	2.23	3-Heptadecen-5-yne, (Z)-
29.09	2.27	Isocyclocitral
29.25	2.27	Cyclopentanol, 3-methyl-2-(2-pentenyl)-
29.92	2.27	1H-Indene, 1-ethylideneoctahydro-, trans-
30.42	1.92	Benzene, 1-methyl-4-(1-methylpropyl)-
31.00	1.92	Benzene, 1-methyl-4-(1-methylpropyl)-
31.42	1.88	Benzene, 1-methyl-2-(2-propenyl)-
32.09	1.88	Benzene, 2-ethenyl-1,4-dimethyl-
32.42	0.80	Phenol
32.75	1.08	Phenol
33.92	1.96	Naphthalene, 1,2,3,4-tetrahydro-1-methyl-
34.09	1.92	1H-Indene, 2,3-dihydro-4,6-dimethyl-
34.34	1.88	Naphthalene, 1,2,3,4-tetrahydro-1-methyl-
35.09	0.92	Phenol, 2-methyl-

35.84	1.12	Phenol, 3,4-dimethyl-, acetate
36.42	1.92	Naphthalene, 1,2,3,4-tetrahydro-1-methyl-
36.42	1.64	Azulene
37.25	0.84	p-Cresol
38.75	1.92	Naphthalene, 1,2,3,4-tetrahydro-6-methyl-
39.67	1.20	Phenol, 3-(1-methylethyl)-
39.67	1.96	Naphthalene, 5-ethyl-1,2,3,4-tetrahydro-
40.67	1.24	Phenol, 3-ethyl-5-methyl-
41.50	1.04	Phenol, 2-ethyl-
41.84	1.96	Naphthalene, 6-ethyl-1,2,3,4-tetrahydro-
42.00	0.92	Phenol, 4-ethyl-
42.25	1.28	Phenol, 2-ethyl-4-methyl-
42.50	1.72	Naphthalene, 2-methyl-
43.00	1.32	Phenol, 3,5-diethyl-
43.34	1.72	1H-Indene, 1-ethylidene-
43.42	1.08	Phenol, 2-ethyl-4-methyl-
44.09	1.28	Phenol, 3,5-diethyl-
44.34	1.12	Phenol, 2-ethyl-4-methyl-
44.50	1.32	Thymol
44.75	1.00	Phenol, 3-(1-methylethyl)-
45.00	1.28	Phenol, 2-ethyl-4,5-dimethyl-
45.50	1.12	Phenol, 3-(1-methylethyl)-
45.84	1.12	Phenol, 2,4,6-trimethyl-
45.84	1.32	Thymol
46.09	1.04	Phenol, 3-(1-methylethyl)-
46.42	1.00	Phenol, 2-propyl-
46.84	1.72	Biphenyl
47.00	1.40	2-Ethyl-5-n-propylphenol
47.42	1.16	2,5-Diethylphenol
47.50	1.80	Naphthalene, 2-ethyl-
47.59	1.16	Phenol, 3,4,5-trimethyl-
47.92	1.36	2-Ethyl-5-n-propylphenol
47.92	1.12	Phenol, 3,5-diethyl-
48.42	1.16	Phenol, 4-(1-methylpropyl)-
49.25	1.08	Thymol
50.00	1.16	Phenol, 3,5-diethyl-
50.17	1.08	Phenol, 3-methyl-6-propyl-
50.92	1.04	Benzene, 1,3-dimethyl-5-(1-methylethyl)-
53.00	1.08	Phenol, p-(2-methylallyl)-
53.50	1.16	1-Butyn-3-one, 1-(6,6-dimethyl-1,2-epoxycyclohexyl)-
54.34	1.12	1(2H)-Naphthalenone, 3,4,4a,7,8,8a-hexahydro-2-hydroxy-8,8-dimethyl-, (2α,4aß,8aß)-
55.67	1.24	6-Hydroxy-4,4,7a-trimethyl-5,6,7,7a-tetrahydrobenzofuran-2(4H)-one
58.09	2.00	Bicyclo[4.4.0]dec-2-ene-4-ol, 2-methyl-9-(prop-1-en-3-ol-2-yl)-
58.25	1.20	Phenol, 4-cyclopentyl-
58.42	2.04	7-Hydroxy-6,9a-dimethyl-3-methylene-decahydro-azuleno[4,5-b]furan-2,9-dione
58.42	1.24	Phenol, 2-(2-penten-4-yl)-4-methyl-
58.84	1.28	Benzofuran, 2,3-dihydro-2,2,4,6-tetramethyl-
59.17	1.44	Phenol, 2-(2-penten-4-yl)-4-methyl-
59.25	1.68	1,1'-Biphenyl, 2-methyl-
59.84	2.04	1,3,5-Cycloheptatriene, 2,5-bis(tetrahydropyranyloxymethyl)-7,7-dimethyl-

59.92	1.32	(1R,3aS,5aS,8aR)-1,3a,4,5a-Tetramethyl-1,2,3,3a,5a,6,7,8-octahydrocyclopenta[c]pentalene
60.09	1.44	Benzene, 1,2,4,5-tetraethyl-
60.42	1.12	Phenol, 4-cyclopentyl-
60.67	1.92	s-Indacene, 1,2,3,5,6,7-hexahydro-4,8-dimethyl-
60.92	1.32	2-(3-Isopropyl-4-methyl-pent-3-en-1-ynyl)-2-methyl-cyclobutanone
62.25	1.52	1-(2-Methoxymethyl-3,5,6-trimethylphenyl)ethanol
62.42	2.00	5,8,11-Heptadecatriynoic acid, methyl ester
62.50	1.36	Benzene, ethylpentamethyl-
62.50	1.44	Phenol, 2-(2-penten-4-yl)-4-methyl-
63.09	1.36	Benzene, 1-ethyl-3,5-diisopropyl-
63.84	1.40	Benzene, 1,2,4,5-tetraethyl-
64.25	1.80	5,8,11,14-Eicosatetraynoic acid
64.42	1.80	1,7-Dimethyl-3-phenyltricyclo[4.1.0.0(2,7)]hept-3-ene
64.50	2.08	Cyclopropane, 1-ethoxy-2,2-dimethyl-3-(2-phenylethenylidene)-
64.50	1.40	Phenol, 2-(1,1-dimethyl-2-propenyl)-3,6-dimethyl-
64.84	1.52	Benzene, 1,2,4,5-tetraethyl-
65.09	2.08	1,8,15,22-Tricosatetrayne
65.25	1.84	1,7-Dimethyl-3-phenyltricyclo[4.1.0.0(2,7)]hept-3-ene
65.42	1.40	Benzene, 1-ethyl-3,5-diisopropyl-
65.42	1.80	Phenanthrene, 1,2,3,4-tetrahydro-
65.50	1.60	δ-Selinene
66.09	1.40	2H-2,4a-Methanonaphthalene, 1,3,4,5,6,7-hexahydro-1,1,5,5-tetramethyl-, (2S)-
66.17	1.60	1,3a-Ethano-3aH-indene, 1,2,3,6,7,7a-hexahydro-2,2,4,7a-tetramethyl-, [1R-(1α,3aα,7aα)]-
66.50	1.44	Benzene, 1-ethyl-3,5-diisopropyl-
66.50	1.64	3H-3a,7-Methanoazulene, 2,4,5,6,7,8-hexahydro-1,4,9,9-tetramethyl-, [3aR-(3aα,4ß,7α)]-
66.59	2.23	3α,17ß-dihydroxyestr-4-ene
66.92	1.44	1R,4R,7R,11R-1,3,4,7-Tetramethyltricyclo[5.3.1.0(4,11)]undec-2-ene
67.17	1.44	Naphthalene, 1,2,4a,5,8,8a-hexahydro-4,7-dimethyl-1-(1-methylethyl)-, (1α,4aß,8aα)-(±)-
67.34	2.04	Cycloisolongifolene, 8,9-dehydro-9-vinyl-
67.92	1.48	Benzene, 1-ethyl-3,5-diisopropyl-
67.92	1.72	2,2,7,7-Tetramethyltricyclo[6.2.1.0(1,6)]undec-4-en-3-one
69.17	1.64	2,3-2H-Benzofuran-2-one, 3,3,4,6-tetramethyl-
69.42	1.48	3H-3a,7-Methanoazulene, 2,4,5,6,7,8-hexahydro-1,4,9,9-tetramethyl-, [3aR-(3aα,4ß,7α)]-
69.75	2.20	Cyclopropa[3,4]cyclohepta[1,2-a]naphthalene, 1,1a,1b,2,3,7b,8,9,10,10a-decahydro-5-methoxy-10-methylene-
69.75	1.68	3,4-2H-Coumarin, 4,4,5,6,8-pentamethyl-
73.09	2.27	Retinol, acetate
74.25	2.31	7-Isopropyl-1,1,4a-trimethyl-1,2,3,4,4a,9,10,10a-octahydrophenanthrene

Table S4b. C_3-C_6 hydrocarbon compounds in liquefied phase identified via 1D GC analysis.

Retention Time	Identified compound
3.466	Propane
3.566	Butane
3.818	Pentane
4.234	Cyclopentane
4.431	n-hexane

Table S4c. Product selectivity's for reductive liquefaction (340°C over MoO_x-Al_2O_3 variants) based on the components identified GCMS.

	Blank	4MoAl	8MoAl	12MoAl	16MoAl
Cycloalkanes+Alkylbenzenes	1.0	38.7	37.7	37.7	38.87
Alkanes	0.0	13.6	15.8	18.1	19.8
Alkylphenols	13.7	11.7	10.3	8.4	6.8
Alcohols	16.6	19.7	15.3	14.7	11.1
Aldehydye/Ketones/Furans	53.8	5.52	12.5	10.0	10.4
Napthalenes/Indans/Biphenyls/Polyaromatics	0.3	2.2	1.6	2.1	2.2
Other oxygenates	14.6	8.5	6.8	9.0	10.9
Total deoxygenated products	**1.3**	**54.5**	**55.0**	**57.9**	**60.9**

Table S5. Observed vibrations from FTIR analysis

Wavenumber (cm^{-1})	**Vibration**	**Reference**
~3336	Hydroxyl group (O-H) stretching vibration (Stretching) in cellulose/lignin	[16]
~2900	C-H Stretching vibration in methyl, $-CH_2-$ and methoxyl group, ν_{Cal-H}	
~1733, 1738	Hemicellulose-lignin complex via uronic ester group in hemicellulose. C=O stretch vibration in hemicelluloses	[16, 17]
~1600, ~1510, and 1419	Aromatic ring vibration (phenylpropane, C9 skeleton),$\nu_{Car=Car}$	[18-20]
1456	C-H deformation (bending) vibration (δ_{Cal-H}) in methyl, methylene, and methoxyl groups	[17, 21]
1365	Vibration of δ_{O-CH3} and $\delta_{C-H,}$ C-H deformation in cellulose/hemicellulose	[16, 17, 21]
1261, 1229,1029	C-O stretching (or alkoxy C-O stretching) vibration of cellulose, hemicellulose or lignin.	[17, 19, 21]
1160	C-H stretching vibration	[17]
1054	Characteristic C–O–C vibration of pyranose ring	[22]
1032	C_{ar}–H in-plane deformation of guaiacyl unit	[23]
~897	Represent the cellulosic beta-glycosidic linkage	[22]

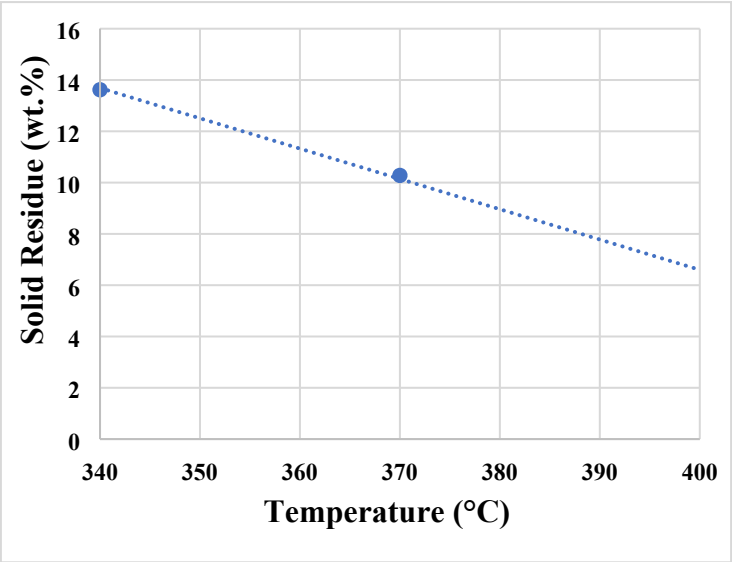

Fig.S6. Effect of temperature on the solid residue formation with 8MoAl catalyst.

Based on the reactivity and catalyst characterization, the catalyst 8MoAl was found optimal. Therefore, a variant of noble and transition metal has been impregnated using 8MoAl as the base catalyst. Table S4 shows their compositions measured by ICP-SFMS and the solid residue obtained after the reductive liquefaction process in the reactor. Based on solid residue content, no promotional activities were obtained for both noble/transition metal impregnation to 8MoAl.

Table S6. Metal contents of the XMo-γAl_2O_3 synthesized catalysts and the solid residue obtained after the reductive liquefaction at 340°C, 35 bar@25°C, 1000 rpm, 4 h, 3:1 ratio

Catalyst	**Elemental composition (wt. %)**			**Solid residue, wt. %**
	X* (wt.%)	Mo (wt. %)	Molar ratio X/(X+Mo)	
γAl_2O_3				23.4
Mo/Al_2O_3	-	8.0	-	13.6
PdMo/Al_2O_3	0.5	8.6	0.05	14.3
PtMo/Al_2O_3	1.1	8.4	0.06	15.6
ReMo/Al_2O_3	0.7	8.0	0.04	16.2
RuMo/Al_2O_3	0.5*	8.7	0.05	16.9
NiMo/Al_2O_3	1.8	7.8	0.27	21.7
CoMo/Al_2O_3	1.9	8.1	0.28	14.7

*X=Pd, Pt, Re, Ni; Co and Mo content were measured by ICP-SFMS. Ru content is shown as-synthesized.

References

[1] A. Farooq, S. Shuing Lam, J. Jae, M. Ali Khan, B.-H. Jeon, S.-C. Jung, Y.-K. Park, Jet fuel-range hydrocarbons generation from the pyrolysis of saw dust over Fe and Mo-loaded HZSM-5(38) catalysts, Fuel 333 (2023). https://doi.org/10.1016/j.fuel.2022.126313.

[2] J. Shi, L. Sun, H. Yan, J. Wang, Catalytic Hydrotreatment of Pine Sawdust Hydropyrolysis Vapor over Ni, Mo-Impregnated HZSM-5 for Optimal Production of Gasoline Components, Energy & Fuels 36(2) (2021) 932-944. https://doi.org/10.1021/acs.energyfuels.1c03271.

[3] Y. Huang, L. Wei, Z. Crandall, J. Julson, Z. Gu, Combining Mo–Cu/HZSM-5 with a two-stage catalytic pyrolysis system for pine sawdust thermal conversion, Fuel 150 (2015) 656-663. https://doi.org/10.1016/j.fuel.2015.02.071.

[4] Q. Cao, C. Zhou, C. Zhong, L.e. Jin, Bio-oil upgraded by catalytic co-pyrolysis of sawdust with tyre, International Journal of Oil, Gas and Coal Technology 8(2) (2014) 235-250.
[5] F. Miao, Z. Luo, Q. Zhou, L. Du, W. Zhu, K. Wang, J. Zhou, Study on the reaction mechanism of C8+ aliphatic hydrocarbons obtained directly from biomass by hydropyrolysis vapor upgrading, Chem. Eng. J. 464 (2023). https://doi.org/10.1016/j.cej.2023.142639.
[6] K. Murugappan, C. Mukarakate, S. Budhi, M. Shetty, M.R. Nimlos, Y. Román-Leshkov, Supported molybdenum oxides as effective catalysts for the catalytic fast pyrolysis of lignocellulosic biomass, Green Chem. 18(20) (2016) 5548-5557. https://doi.org/10.1039/c6gc01189f.
[7] S. Budhi, C. Mukarakate, K. Iisa, S. Pylypenko, P.N. Ciesielski, M.M. Yung, B.S. Donohoe, R. Katahira, M.R. Nimlos, B.G. Trewyn, Molybdenum incorporated mesoporous silica catalyst for production of biofuels and value-added chemicals via catalytic fast pyrolysis, Green Chem. 17(5) (2015) 3035-3046.
[8] A. Eschenbacher, A. Saraeian, B.H. Shanks, P.A. Jensen, C. Li, J.Ø. Duus, A.B. Hansen, U.V. Mentzel, U.B. Henriksen, J. Ahrenfeldt, A.D. Jensen, Enhancing bio-oil quality and energy recovery by atmospheric hydrodeoxygenation of wheat straw pyrolysis vapors using Pt and Mo-based catalysts, Sustainable Energy & Fuels 4(4) (2020) 1991-2008. https://doi.org/10.1039/c9se01254k.
[9] K. Wang, D.C. Dayton, J.E. Peters, O.D. Mante, Reactive catalytic fast pyrolysis of biomass to produce high-quality bio-crude, Green Chem. 19(14) (2017) 3243-3251. https://doi.org/10.1039/c7gc01088e.
[10] Z. Yang, A. Kumar, A.W. Apblett, A.M. Moneeb, Co-Pyrolysis of torrefied biomass and methane over molybdenum modified bimetallic HZSM-5 catalyst for hydrocarbons production, Green Chem. 19(3) (2017) 757-768. https://doi.org/10.1039/c6gc02497a.
[11] M.W. Nolte, J. Zhang, B.H. Shanks, Ex situ hydrodeoxygenation in biomass pyrolysis using molybdenum oxide and low pressure hydrogen, Green Chem. 18(1) (2016) 134-138. https://doi.org/10.1039/c5gc01614b.
[12] V.K. Venkatakrishnan, W.N. Delgass, F.H. Ribeiro, R. Agrawal, Oxygen removal from intact biomass to produce liquid fuel range hydrocarbons via fast-hydropyrolysis and vapor-phase catalytic hydrodeoxygenation, Green Chem. 17(1) (2015) 178-183.
[13] X. Gong, J. Sun, X. Xu, B. Wang, H. Li, F. Peng, Molybdenum-catalyzed hydrogenolysis of herbaceous biomass: A procedure integrated lignin fragmentation and components fractionation, Bioresour. Technol. 333 (2021) 124977. https://doi.org/10.1016/j.biortech.2021.124977.
[14] M. Grilc, B. Likozar, J. Levec, Hydrodeoxygenation and hydrocracking of solvolysed lignocellulosic biomass by oxide, reduced and sulphide form of NiMo, Ni, Mo and Pd catalysts, Appl. Catal., B 150-151 (2014) 275-287. https://doi.org/10.1016/j.apcatb.2013.12.030.
[15] M. Grilc, B. Likozar, J. Levec, Simultaneous Liquefaction and Hydrodeoxygenation of Lignocellulosic Biomass over NiMo/Al_2O_3, Pd/Al_2O_3, and Zeolite Y Catalysts in Hydrogen Donor Solvents, ChemCatChem 8(1) (2016) 180-191. https://doi.org/10.1002/cctc.201500840.
[16] G. Zhu, X. Xing, J. Wang, X. Zhang, Effect of acid and hydrothermal treatments on the dye adsorption properties of biomass-derived activated carbon, Journal of Materials Science 52(13) (2017) 7664-7676. https://doi.org/10.1007/s10853-017-1055-0.
[17] G. Charis, G. Danha, E. Muzenda, Characterizations of Biomasses for Subsequent Thermochemical Conversion: A Comparative Study of Pine Sawdust and Acacia Tortilis, Processes 8(5) (2020). https://doi.org/10.3390/pr8050546.
[18] M.N.M. Ibrahim, A. Iqbal, C.C. Shen, S.A. Bhawani, F. Adam, Synthesis of lignin based composites of TiO2 for potential application as radical scavengers in sunscreen formulation, BMC Chem 13(1) (2019) 17. https://doi.org/10.1186/s13065-019-0537-3.
[19] F. Kong, K. Parhiala, S. Wang, P. Fatehi, Preparation of cationic softwood kraft lignin and its application in dye removal, Eur. Polym. J. 67 (2015) 335-345. https://doi.org/10.1016/j.eurpolymj.2015.04.004.

[20] P. Yan, Z. Xu, C. Zhang, X. Liu, W. Xu, Z.C. Zhang, Fractionation of lignin from eucalyptus bark using amine-sulfonate functionalized ionic liquids, Green Chem. 17(11) (2015) 4913-4920. https://doi.org/10.1039/c5gc01035g.
[21] B. Joffres, C. Lorentz, M. Vidalie, D. Laurenti, A.A. Quoineaud, N. Charon, A. Daudin, A. Quignard, C. Geantet, Catalytic hydroconversion of a wheat straw soda lignin: Characterization of the products and the lignin residue, Appl. Catal., B 145 (2014) 167-176. https://doi.org/10.1016/j.apcatb.2013.01.039.
[22] M. Thakur, A. Sharma, V. Ahlawat, M. Bhattacharya, S. Goswami, Process optimization for the production of cellulose nanocrystals from rice straw derived α-cellulose, Materials Science for Energy Technologies 3 (2020) 328-334. https://doi.org/10.1016/j.mset.2019.12.005.
[23] A. Jablonskis, A. Arshanitsa, A. Arnautov, G. Telysheva, D. Evtuguin, Evaluation of Ligno Boost™ softwood kraft lignin epoxidation as an approach for its application in cured epoxy resins, Industrial Crops and Products 112 (2018) 225-235. https://doi.org/10.1016/j.indcrop.2017.12.003.